Global J. Environ. Sci. Manage. 9(3): 389-402, Summer 2023, Serial #35

Global Journal of Environmental Science and Management
(GJESM)

Homepage: https://www.gjesm.net/

Podcasts

ORIGINAL RESEARCH PAPER

Relationship between chlorophyll-a, sea surface temperature and sea surface salinity

M.N. Hidayat[1,2], R. Wafdan[3], M. Ramli[2], Z.A. Muchlisin[1,4,5], S. Rizal[1,3,5]

[1] *Graduate School of Mathematics and Applied Sciences, Universitas Syiah Kuala, Banda Aceh 23111, Indonesia*

[2] *Department of Mathematics, Universitas Syiah Kuala, Banda Aceh 23111, Indonesia*

[3] *Department of Marine Sciences, Faculty of Marine and Fisheries, Universitas Syiah Kuala, Banda Aceh, 23111, Indonesia*

[4] *Department of Aquaculture, Faculty of Marine and Fisheries, Universitas Syiah Kuala, Banda Aceh 23111, Indonesia*

[5] *Research Center for Marine Sciences and Fisheries, Universitas Syiah Kuala, Banda Aceh 23111, Indonesia*

ARTICLE INFO

Article History:
Received 11 October 2022
Revised 12 November 2022
Accepted 22 December 2022

Keywords:
Coefficient of correlation
Copernicus Marine Environment Monitoring Service (CMEMS Data)
Northern Bay of Bengal
Northeast monsoon
Seasonal model
Southwest monsoon

DOI: 10.22035/gjesm.2023.03.03

ABSTRACT

BACKGROUND AND OBJECTIVES: This study aimed to investigate the long-term relationship between chlorophyll-a, sea surface temperature, and sea surface salinity monthly from January 2015 to December 2021. It was carried out in the Northern Bay of Bengal, which experiences extreme monsoons, in the southwest monsoon and northeast monsoon from June to September and November to February, respectively. Monsoon is the main cause of changes in chlorophyll-a, sea surface temperature and sea surface salinity.

METHODS: The seasonal model was used to examine the relationship between these three parameters, which were obtained using the Copernicus Marine Environment Monitoring Service data. The seasonal model was used to observe periodic patterns and predict parameters based on their regularity. Meanwhile, Pearson's correlation analysis was conducted to determine the relationship between chlorophyll-a, sea surface temperature and sea surface salinity.

FINDINGS: This study found that the three parameters, namely chlorophyll-a, sea surface temperature, and sea surface salinity, follow the monsoon pattern, as shown in the seasonal model. The minimum value of chlorophyll-a occurred in February, March and April, while the maximum value of approximately 2 milligram per cubic meter occured at stations 1, 2, 3, 4, 5 and 7, but at 9 and 10, it increased to 12-14 mg/m3. This indicates that station positions are very sensitive to changes in chlorohophyll-a values. When the southwest monsoon occurred, it reached the maximum. Furthermore, the minimum sea surface temperature values occurred in January and at almost every station in the year. It was shown to be associated with the northeast monsoon, which causes winter. On the sea surface temperature graph, several peaks were observed in positive local extremes yearly at almost all stations. The maximum sea surface temperature occurred in May, June, and July, according to the shape of the graph, which peaked in the middle of the year. The sea surface salinity graph formed a peak and valley which occurred yearly in May or April, as well as September and October, respectively.

CONCLUSION: Chlorophyll-a had 1 trough and 1 peak, with the sea surface temperature graph possessing only 1 peak, while the sea surface salinity graph had 1 peak and 1 trough, respectively. These graph patterns implied that chlorophyll-a first achieved a minimum value before reaching the máximum. The sea surface temperature graph had a maximum value in the middle of the year, while the minimum occurred at the beginning or end. Moreover, the sea surface salinity graph first reached the maximum value and then declined to the minimum.

NUMBER OF REFERENCES	NUMBER OF FIGURES	NUMBER OF TABLES
38	5	4

*Corresponding Author:
Email: *srizal@unsyiah.ac.id*
Phone: + 628 52571 49009
ORCID: 0000-0003-3637-2351

Note: Discussion period for this manuscript open until October 1, 2023 on GJESM website at the "Show Article".

INTRODUCTION

The Bay of Bengal (BoB) is bordered by the Indian subcontinent, Southeast Asia, and the northern Indian Ocean, with a complex bathymetry, as shown in Fig. 1. Generally, the climate in the Northern BoB (NBoB) is dominated by monsoons. The Northeast (NE) monsoon occurs from November to February and the Southwest (SW) monsoon from June to September (Goswami *et al.*, 2016). Fig. 2 shows the wind pattern in February and August 2021, which sequentially emerges from the NE and SW. The magnitude of wind stress is two times greater in August than in February. The average wind speed in August and February is approximately 6.3 meter per second (m/s) and 7 m/s, respectively.

According to Miranda *et al.* (2021), water quality variability in the NBoB is greatly influenced by the following factors, SW and NE monsoons which change seasonally, waste disposal from rivers and various industries on the coast, as well as frequent tropical cyclone (TC) events. Since the global thermohaline circulation is driven by density, it is paramount to study the relationship between sea surface salinity (SSS), sea surface temperature (SST), and chlorophyll-a (Chl-a). This is formed by salinity and temperature, the basic physical properties of seawater and the main drivers of global climate dynamics. These properties also affect oceanic biogeochemical cycles and the atmospheric carbon flux (Woolf *et al.*, 2016). As an important variable in climate change, SSS and SST strongly influence the hydrological cycle. (Belward *et al.*, 2016) stated that anthropogenic climate change tends to respond to the hydrological cycle. Some tracer in ocean circulation is determined by SSS, thereby making it an important factor in climate change (Bosc *et al.*, 2009). An extremely close relationship exists in the tropical Pacific between SSS and SST, which is detected through hydrodynamic processes (Zheng and Zhang, 2015). For example, as an external driver, the following factors SSS, density, and oceanic stratification are affected by freshwater flux, which tends to affect SST (Zhang and Busalacchi, 2009). El Niño-Southern Oscillation (ENSO) variability is caused by the SSS and SST anomalies near the dateline, characterized by its evolution (Qi *et al.*, 2019). According to Sahoo and Bhaskaran (2015), the observations made in BoB during 1998, 2001, 2005, and 2013 proved that there is a positive relationship between SST and cyclones. High SST results were found in extreme cyclone intensity, and concerning salinity, there has been a negative relationship between the upper oceanic stratification and post-monsoon TC intensification for the past two decades. TC tends to strengthen when this variable is low (Fan *et al.*, 2020). The depiction of cyclones in BoB over a long period (1877 to 2016) was documented by Bandyopadhyay *et al.* (2021). A positive relationship exists between its intensity and Chl-a concentration (Latha *et al.*, 2015). The impact of the spatiotemporal evolution of SSS needs to be studied because it closely connects with climate variability (Eyring *et al.*, 2016). The concentration of Chl-a and its primary productivity are affected by light penetration caused by the formation of a gradient due to SSS and SST, which is closely related to the distribution of nutrients and suspended sediments (Torregroza-Espinosa, 2021). Björn *et al.* (2009) stated that light harvesting and the conversion of an absorbed photon into chemical energy are two important and irreplaceable roles of Chl-a in oxygenic photosynthesis. Li *et al.* (2018) observed the leaves of 823 plant species and discovered that Chl-a, chlorophyll-b (Chl-b), and chlorophyll-a per chlorophyll-b (Chl-a/b) have an average value of 4.18 milligram per gram (mg/g), 1.72 mg/g and 2.47 mg/g, respectively. The study was conducted in nine Chinese forest communities from cold to tropical zones. In this circumstance, it appears that the value of Chl-a is greater than Chl-b. Li *et al.* (2018) categorized plant functional groups based on different Chl. It was reported that trees have lower Chl values than shrubs and herbs. Coniferous and evergreen trees have lower Chl values than broadleaved and deciduous ones. Some other studies reported that Chl-a, Chl-b, and total chlorophyll (Chl a+b) increase with higher latitude. In 2015 and 2016, seasonal changes, such as the SW and NE monsoons in NBoB, greatly affected the interannual variations of SST, SSS, and Chl-a (Dutta and Paul, 2021). During the NE and SW monsoons, NBoB becomes cool and relatively warm, respectively. This is in accordance with the observations conducted by Sarangi and Devi (2017). The SW and NE monsoons also affect SST variability and Chl-a production (Vecchi and Harrison, 2002). Choudhury and Pal (2010) reported that during the SW monsoon, SSS decreases due to the large discharge of fresh water from the Ganges and Brahmaputra rivers flowing into NBoB. There is an increase in SSS on the coastal periphery, which

positively correlates with a rise in phytoplankton production during the NE monsoon. During the rainy season, there is also an increase in the NBoB turbidity. Chauhan *et al.* (2005) reported a reduction of light penetration in the water column, which negatively impacts Chl-a production in the region. Several studies utilized the Copernicus Marine Environment data portal Monitoring Service (CMEMS). For instance, including Ikhwan *et al.* (2022) researched to determine mixed layer depth (MLD) using CMEMS salinity data. Similarly, Pisano *et al.* (2020) studied long-term oceanic variability with SST data, while Moradi (2021) tested the accuracy of Chl-a concentrations using in situ data collected from 2008 to 2018. Excellent results were obtained by comparing the CMEMS model and the concentration of float Chl-a (Biogeochemical-Argo (BGC-Argo), measurements data). This was indicated by a correlation coefficient and root mean square error (RMSE) of 0.81 and 0.59, respectively (Lamouroux *et al.*, 2019). Exceptional results were also obtained by comparing three-dimensional (3D) temperature data (in Kelvin) with in situ observation data at a depth of 0 to 5 meter (m). This was reflected by the root mean square (RMS), which comprises in situ thematic centre (INS TAC), which had a value of 0.65, and for Indian Ocean data on comparison with in situ CORIOLIS, having a value of 0.44. The comparison of 3D salinity data (in practical salinity unit (psu)) with in situ observational data showed excellent results. The RMS value at a depth of 0 to 5 m for global and Indian Ocean data was 0.65 and 0.204, respectively (Lellouche *et al.*, 2019). This present study was conducted to examine the relationship between Chl-a, SST, and SSS parameters monthly from January 2015 to December 2021. A total of 10 stations were selected in NBoB, as shown in Fig. 1 and Table 1. This process was achieved using the following three steps, namely 1) The graphs of the three parameters, including Chl-a, SST, and SSS for all stations, were plotted, 2) These led to the derivation of the seasonal model at all stations, 3) The correlations between Chl-a and SST, Chl-a and SSS, as well as SST and SSS at all stations were also obtained. Based on the literature review, the monthly long-term relationship between Chl-a, SST, and SSS in NBoB using the seasonal model and the correlation method has never been carried out. The seasonal model was used to analyze the behavior of Chl-a, SST, and SSS and the possible prediction of these three parameters. This present study is extremely relevant because it relates to the fisheries sector. This is caused by the monsoon, which plays an important role in the Chl-a cycle alongside, its interaction with SST and SSS in NBoB. According to Dutta and Paul (2021), this also influences the variability of the fish assemblage. Monsoons also affect the availability of nutrients in the upper layer of NBoB and trigger phytoplankton's expansion (Vinayachandran *et al.*, 2005). The diversity and composition of reef fish depend highly on SST, coral richness, shelf width, and Chl-a (Floeter *et al.*, 2001). Daqamseh *et al.* (2019) conducted study in the Red Sea and reported a correlation between Chl-a, SST, and SSS. Higher SSS and warmer SST coupled with lower Chl produce an uncomfortable environment for fish to live in. This study aims to investigate the long-term relationship between chlorophyll-a, sea surface temperature, and sea surface salinity in the northern Bay of Bengal, situated in India, Bangladesh, and Myanmar, monthly from January 2015 to December 2021.

MATERIALS AND METHODS

This present study was conducted in NBoB, located at coordinates 18°N to 24.6°N and 85°E to 95°E, and it focused on 10 stations, as shown in Table 1. The visualization for the stations studied is clearly shown in Fig. 1. The data used were monthly reports on Chl-a, SST, and SSS (Lellouche *et al.*, 2018). It was obtained from the Copernicus Marine Environment data portal Monitoring Service (CMEMS) website (Le Traon *et al.*, 2019). Meanwhile, the other data used included wind per 6 hours obtained from the National Centers for Environmental Prediction (NCEP)/National Center for Atmospheric Research (NCAR) reanalysis 1 (Kalnay *et al.*, 1996).

Seasonal model

Seasonal models aim to identify seasonal patterns and predict parameters based on regularity (Ikhwan *et al.*, 2022). Chl-a, SST, and SSS data were analyzed using this framework based on non-linear regression as stated in Eq. 1 (Haridhi *et al.*, 2016):

$$y = \alpha + \beta \sin\left(2\pi t\right) + \gamma \cos\left(2\pi t\right) \quad (1)$$

where, α, β, γ and t are the constant vertical displacement, the amplitude of the sine wave, cosine wave, and time, respectively.

Table 1: Study station location

No	Station	Longitude (°E)	Latitude (°N)
1	1	87.25	20.5
2	2	89	20.75
3	3	87.25	21
4	4	88	21
5	5	89	21
6	6	90	21
7	7	88.5	21.5
8	8	89.75	21.5
9	9	91	21.5
10	10	91.75	22

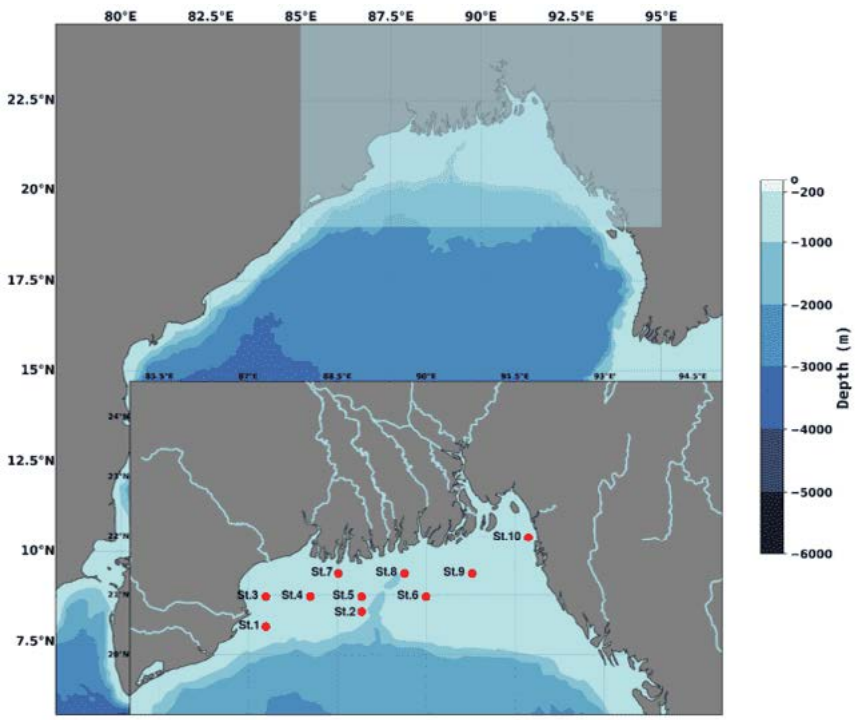

Fig. 1: Bathymetrical location of the study area in NBoB and the sample station (red dot). The map was plotted using Natural Earth raster + vector data (naturalearthdata.com). The blue color difference indicates the depth (m).

Correlation analysis

Pearson's correlation analysis was used to evaluate the relationship between Chl-a - SST, Chl-a - SSS, and SST - SSS. The correlation equation and coefficient used are stated in Eqs. 2 and 3 (Haditiar *et al.*, 2019).

$$y = b + ax, \tag{2}$$

$$R = \frac{\sum(x_i - \bar{x})(y_i - \bar{y})}{\sqrt{\sum(x_i - \bar{x})^2 \sum(y_i - \bar{y})^2}}. \tag{3}$$

Where $b, a, R,$ are the y-intercept constant, slope of the regression line (regression coefficient), and

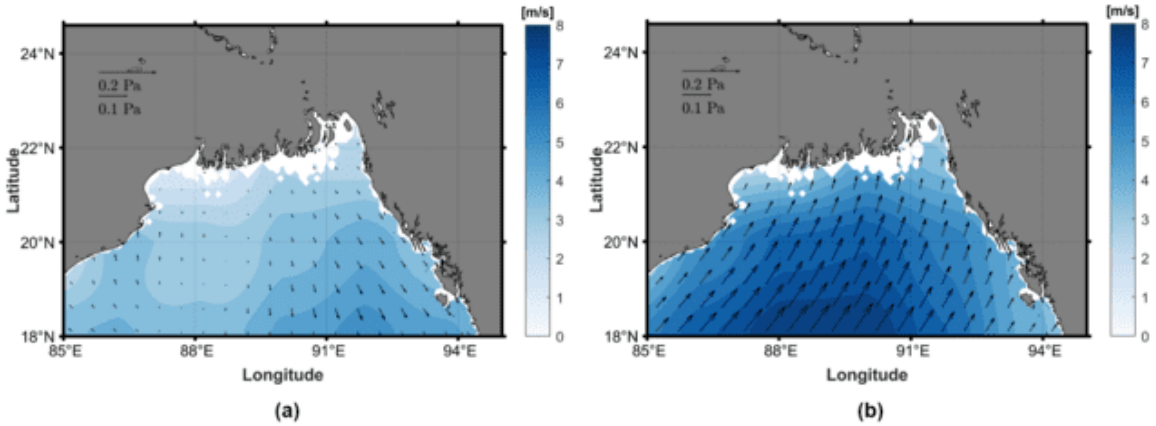

Fig. 2: The wind velocity (color in m/s) and wind stress (arrow in Pascals (Pa)) in (a) February and (b) August 2021, derived from NCEP/NCAR

correlation coefficient, respectively. The variables x_i and y_i are used to calculate the correlation coefficient between Chl-a and SST, Chl-a and SSS, as well as SST and SSS, where i is the corresponding data index, $\overline{x}$, and $\overline{y}$ is the average sample data of each station.

RESULTS AND DISCUSSION

Chlorophyll-a (Chl-a), sea surface temperature (SST), and sea surface salinity (SSS)

Fig. 3a, b, and c show the Chl-a, SST, and SSS, respectively, at stations 1 to 10 for seven years (2015 to 2021). Generally, the curve of Chl-a with respect to time is relatively flat and of low value from January to May, with peaks in different months. The minimum value realized in each year and station tends to differ. For example, in 2015, the minimum value was obtained in January, February, March and April. In 2016, the minimum value of Chl-a was detected in February, March and April. High concentrations of Chl-a occurred at stations 8, 9, and 10, namely between 6 to 14 milligram per cubic meter (mg/m^3). According to Dutta and Paul (2021), its peak reached a relatively 2 mg/m^3. Its domain in NBoB was within the range of 20°20′ to 21°30′ N and 87°30′ to 89° E. These tend to correspond to stations 1, 2, 3, 4, 5, and 7, which had an average Chl-a concentration of relatively 2 mg/m^3. Based on the results obtained, its peak at the earlier-mentioned stations occurred in July, August, and September. According to Dutta and Paul (2021), peak conditions generally occur between October and November. These differences might be because Dutta and Paul (2021) conducted a study on the NBoB in the domains 20°20′ to 21°30′ N and 87°30′ to 89° E in one station, while this present study was performed in 6 stations. Another interesting fact is that at stations 9 and 10, the concentration of Chl-a increased by relatively 12 to 14 mg/m^3, even though it was only 2°30′ E in the longitude direction from the other 8 stations and virtually no difference in the direction of latitude N. This implies that the values of Chl-a in NBoB are extremely sensitive to the positions of these stations, and this in turn has a significant impact on its concentration. Minimum values were detected in January, February, March, and April, while the maximum for all stations was observed in July, August, and September, during the SW monsoon period. Fig. 3b shows the SST values for each year at the 10 stations, in contrast to the relatively flat Chl-a at the beginning. The SST chart moved straight to the peak starting from the beginning of the year and then immediately decreased towards the end. Its minimum values, were detected in virtually every station and January. Occasionally, there was a shift in the minimum SST from January to December and February. This is associated with the NE monsoon, which causes winter. Dutta and Paul (2021) also noted that the minimum SST occurred every January from 2006 to 2015, with values ranging from 25 to 26 degree Celcius (°C). The minimum SST in this study was slightly lower, ranging from 23 – 25° C. Another characteristic of the SST graph is that there were several peaks in the form of positive local extremes every year at virtually all stations. The graph plotted by Dutta and Paul (2021) also showed similar characteristics, namely several positive local extreme

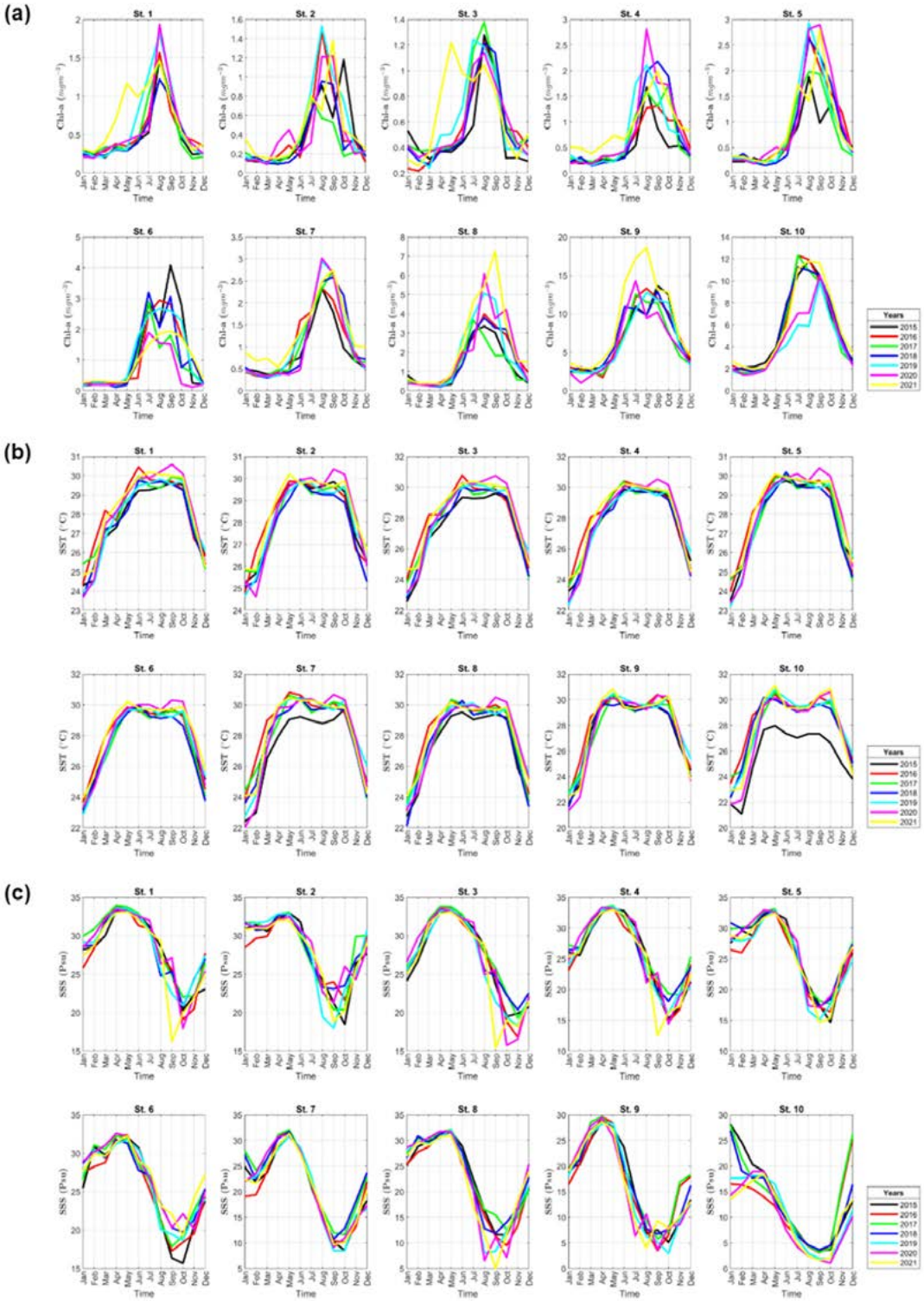

Fig. 3: Data of (a) Chl-a, (b) SST, and (c) SSS from Stations 1 to 10 for seven years (2015 to 2021)

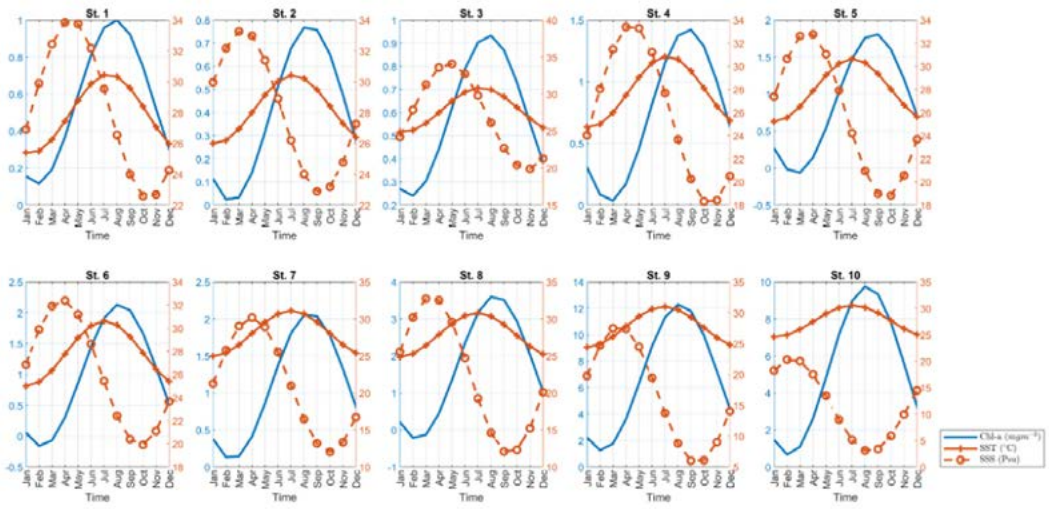

Fig. 4: Seasonal model of Chlorophyll-a (Chl-a) (solid line with blue color, in), Sea Surface Temperature (SST) (solid brown line with a plus symbol, in °C), and Sea Surface Salinity (SSS) (dashed brown line with empty bullets, in psu), with 10 sample station (St. 1-10). The position of the axis values of each graph corresponds to the color of the graph, namely the left ordinate for Chl-a (blue color) and the right ordinate for SST and SSS (brown color).

peaks. Based on Fig. 3b, the maximum SST occurred in May, June, and July, with its peak in the middle of the year. The SSS values from 2015 to 2021 at the 10 stations are shown in Fig. 3c. Its graph formed one peak and trough each year. The peak occurred in May or April, while the trough was observed in September and October. Dutta and Paul (2021) reported that the maximum and minimum values of SSS (34.76 psu) and (13.67 psu), were detected in May 2008 and September 2015, respectively.

Seasonal model

The data acquired from 2015 to 2021, were analyzed using the seasonal model, as shown in Fig. 4. This tool was used to simplify the analysis results at 10 stations, which produced repeated curve annually. The data tabulation in Table 2 summarizes the results obtained with this instrument.

The results of the seasonal model analysis in Eq. 1 are shown in Table 2, which summarizes the values of α, β, and γ for each of the Chl-a, SST, and SSS data. In general, Table 2 shows the behavior of the curves in Fig. 4. The constant α is a value that is not affected by the season, while β and γ are seasonally influenced constants. The average value of α in Table 2 indicates that the largest value for the variable Chl-a occurred at stations 9 and 10, while the least was detected at station 2. For the SST variable, the values of the largest and least constant α were found at stations 2 and 10, respectively. Finally, for the SSS variable, the largest and least values for constant α were found at stations 1 and 10, respectively.

Table 3 shows the peak and trough positions in Fig. 4 for each sample station in this study. The minimum (min) and maximum (max) values for Chl-a at 10 stations occurred in February and March, as well as August and September. The min and max SST values at 10 stations were observed in January and July, respectively. Meanwhile, the values in the SSS data for the 10 stations vary more than the other variables. The min value varied from August to November, while the Max was observed between February and May. Chaturvedi (2005) reported that stations 2 and 6 are consistent, thereby comparing them. The min and max SST was observed from January to February, and in November, respectively (Chaturvedi (2005). This is inconsistent with the results of this present study, where the Max SST occured only in July due to its inability caused by cloud cover from May to September (Chaturvedi, 2005). Furthermore, the Chl-a Max value in this study was obtained in August, while that of Chaturvedi (2005) was min and in November. The NE monsoon prohibited the Chl-a values due to salinity, while in SW the results were high.

Table 2: Constant and coefficient of predictor

No	Station	Chl-a			SST			SSS		
		α	β	γ	α	β	γ	α	β	γ
1	1	0.5577	-0.36477	-0.25254	27.92338	-1.67054	-1.94275	28.2245	4.2192	-3.9558
2	2	0.39621	-0.36212	-0.11621	28.21127	-1.27976	-1.80849	28.0884	5.185	-0.8231
3	3	0.58676	-0.28314	-0.20178	27.858	-1.7856	-2.406	27.002	4.3083	-5.7076
4	4	0.73014	-0.69313	-0.0868	27.8047	-1.7999	-2.4909	25.869	5.6126	-5.3555
5	5	0.873	-0.93425	-0.15681	27.94284	-1.41525	-2.30781	25.8049	6.8179	-2.1178
6	6	0.98587	-1.05471	-0.4609	27.8159	-1.4607	-2.4149	26.1491	5.7571	-2.4962
7	7	1.09303	-0.94727	-0.27758	28.0456	-1.5406	-2.6588	21.1214	7.9253	-4.4066
8	8	1.69226	-1.82073	-0.65607	27.8367	-1.4202	-2.6113	22.4157	10.3219	-2.3255
9	9	6.7795	-5.0123	-2.3524	27.7017	-1.5693	-2.8952	16.7618	10.7283	-2.7278
10	10	5.2156	-4.1246	-1.9426	27.5859	-1.5584	-2.5436	11.7085	8.3152	2.7693

Table 3: Peaks and troughs for the seasonal model

No	Station	Chl-a				SST				SSS			
		Min	Value	Max	Value	Min	Value	Max	Value	Min	Value	Max	Value
1	1	Feb	0.1155	Aug	0.9999	Jan	25.4056	Jul	30.4411	Oct	22.5927	Apr	33.8563
2	2	Feb	0.0245	Aug	0.7679	Jan	26.0052	Jul	30.4173	Sep	22.9034	Mar	33.2734
3	3	Feb	0.2407	Aug	0.9329	Jan	24.8815	Jul	30.8345	Nov	19.9049	May	34.0991
4	4	Mar	0.0370	Sep	1.4233	Jan	24.7476	Jul	30.8618	Oct	18.3306	Apr	33.4074
5	5	Mar	-0.0613	Sep	1.8073	Jan	25.2366	Jul	30.6491	Oct	18.8415	Apr	32.7683
6	6	Feb	-0.1580	Aug	2.1297	Jan	24.9942	Jul	30.6376	Oct	19.9152	Apr	32.3830
7	7	Feb	0.1339	Aug	2.0522	Jan	24.9727	Jul	31.1185	Oct	12.0546	Apr	30.1882
8	8	Feb	-0.2126	Aug	3.5971	Jan	24.8651	Jul	30.8083	Sep	12.0938	Mar	32.7376
9	9	Feb	1.2625	Aug	12.2965	Jan	24.4097	Jul	30.9937	Sep	6.0335	Mar	27.4901
10	10	Feb	0.6723	Aug	9.7589	Jan	24.6039	Jul	30.5679	Aug	3.1227	Feb	20.2943

Correlation analysis

The correlation images of the Chl-a – SST, Chl-a – SSS, and SST – SSS variable pairs for seven years are shown in Fig. 5. However, the tabulated data is shown in Table 4 to facilitate analysis. Fig. 5(a-j) shows the actual data curves of Chl-a, SST, and SSS, which are located in the first column position. The figures in the three consecutive columns explain the correlation between Chl-a – SST, Chl-a – SSS, and SST – SSS data. Based on the results obtained, Chl-a and SST data were shown to have a positive relationship. This is indicated by the slope of the regression line (blue line) that appears at the 10 stations investigated. A positive correlation signifies that the values of Chl-a and SST are directly proportional. This simply implies when the Chl-a value is high at a station, it will offset that of SST and vice versa. The actual data values in the first column, and the trend of the peaks and troughs on Chl-a (orange line), corresponding to the movement on SST. A negative correlation exists between the Chl-a and SSS data, except for the data acquired at station 3 as indicated by the slope of the regression line. The negative correlation suggests that the value comparison between Chl-a

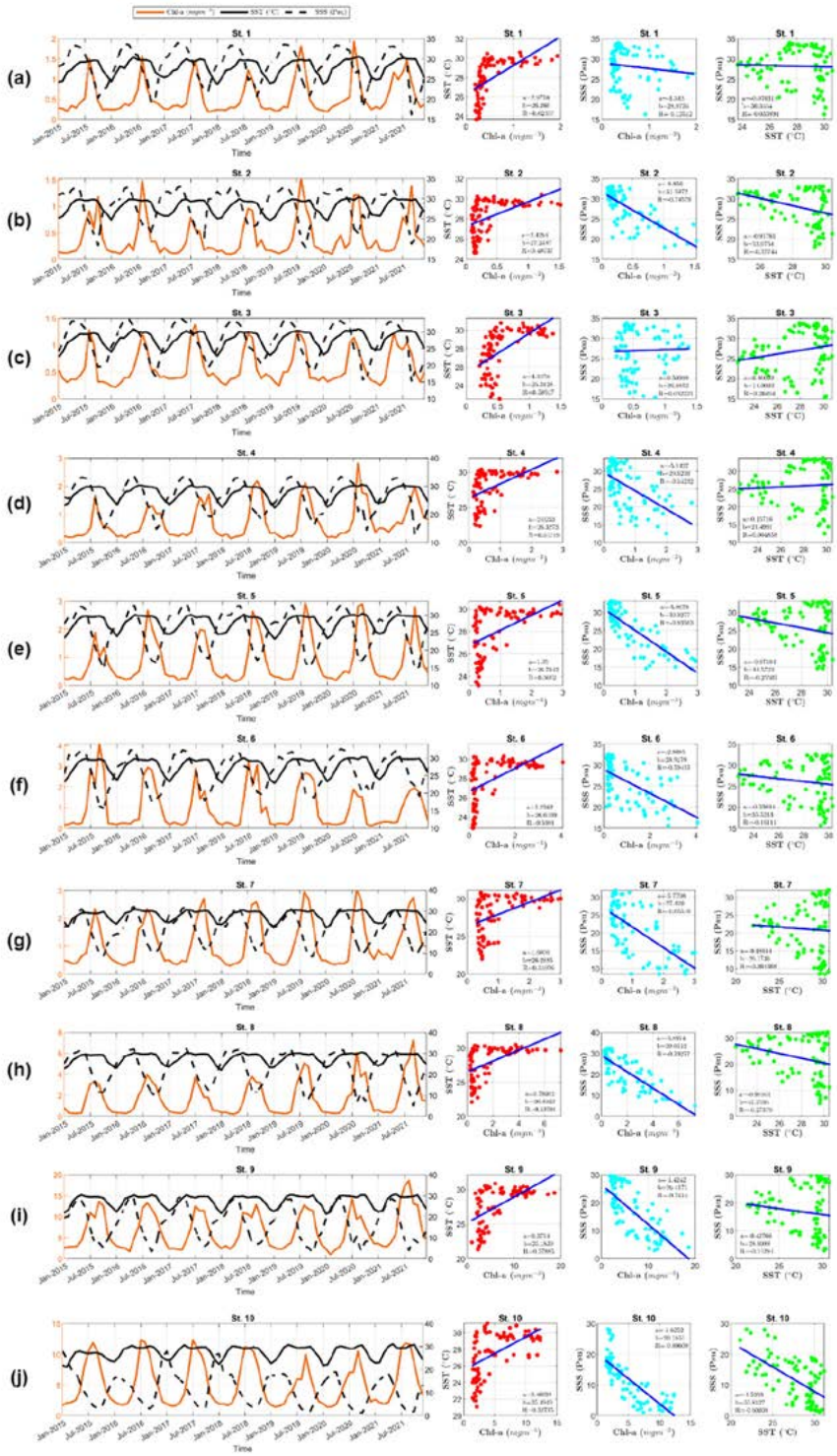

Fig. 5: (First column) Time series of Chl-a concentration (in solid brown line color), SST (in solid black line color), and SSS (in dashed black line) in the 10 stations (St. 1-10), which is marked by (a-j). Correlation analysis for Chl-a and SST (Second column), Chl-a and SSS (Third column), and SST and SSS (Fourth column) in the 10 stations (St. 1-10).

Table 4: Statistical data of all the variables

No	Station	Chl-a - SST			Chl-a - SSS			SST - SSS		
		a	b	R (corr coef)	a	b	R (corr coef)	a	b	R (corr coef)
1	1	2.97	26.27	0.62	-1.34	28.97	-0.13	-0.08	30.36	-0.03
2	2	2.43	27.25	0.50	-8.86	31.60	-0.75	-0.92	53.98	-0.38
3	3	4.34	25.31	0.59	0.54	26.69	0.03	0.47	14.01	0.20
4	4	2.02	26.33	0.52	-5.14	29.62	-0.54	0.16	21.50	0.06
5	5	1.35	26.76	0.51	-5.87	30.93	-0.84	-0.67	44.57	-0.26
6	6	1.22	26.62	0.54	-2.81	28.92	-0.59	-0.34	35.52	-0.16
7	7	1.61	26.29	0.51	-5.77	27.43	-0.66	-0.18	26.17	-0.06
8	8	0.79	26.49	0.54	-3.90	29.01	-0.79	-0.91	47.76	-0.27
9	9	0.37	25.18	0.58	-1.42	26.42	-0.74	-0.43	28.61	-0.14
10	10	0.40	25.49	0.53	-1.63	20.19	-0.81	-1.60	55.81	-0.60

and SSS is inversely proportional. When the Chl-a value is high at a station, that of the SSS tends to have an opposite trend and vice versa. The negative correlation between Chl-a and SSS corresponds to the real data curve in the first column. The Chl-a data curve (orange line) trend is the opposite of the SSS (dashed black line). In this case, the peak of the curve from the Chl-a data corresponds to the trough of the one from SSS. The trough of the curve from the Chl-a data corresponds to the peak of the one from SSS. For the cases encountered at station 3, the slope of the regression line was close to zero, meaning that the linear relationship between these variables is almost non-existent. The peaks and troughs of the Chl-a and SSS data curves do not correspond properly, thereby causing the correlation to be equivalent to zero.

The correlation between SST and SSS data was almost non-linear for stations 1, 4, and 7, while a positive relationship existed at 3. A negative relationship was detected in the remaining stations namely 2, 5, 6, 8, 9, and 10. The slope of the regression line, which was close to 0 at stations 1, 4, and 7, shows that the data varies and tends to spread out, therefore, there is virtually no linear relationship between the SST and SSS variables. The positive slope of the regression line at station 3 indicates that the comparison of SST and SSS values is directly proportional. For instance, when SST is high at this station, SSS will also be extreme, and vice versa. The negative correlation shown by the regression slope at stations 2, 5, 6, 8, 9, and 10 culminated in an inverse relationship between the SST and SSS variables. When the SST value increases, that of the SSS at these stations reduces and vice versa. The three types of relationships that occurred between these variables are described in the actual data curves in the first column of Fig. 5. At stations 1, 4, and 7, the SST and SSS curves were incoherent. In this case, the peaks and troughs of the curves shifted and were out of sync. The curve in station 3 indicates better synchronization as the curves' peaks and troughs appeared parallel, resulting in a positive correlation. A similar phenomenon occurred at stations 2, 5, 6, 8, 9, and 10. The peaks and troughs of SST and SSS appeared to be synchronous. The SST peak aligned with the SSS trough, while the SST trough vertically aligned with the SSS.

A summary of the statistical data from Fig. 5 is shown in Table 4. Schober (2018), stated that the correlation between Chl-a and SST pairs is moderate and positive at all stations, with a value of $0.50 \leq R \leq 0.62$. The relationship is strong and negative for the Chl-a and SSS pairs with a value of $-0.74 \leq R \leq -0.84$ at stations 2, 5, 8, 9, and 10. Meanwhile, at stations 4, 6, and 7, there was a moderate and negative correlation with a value in the range of $-0.54 \leq R \leq -0.66$. A weak and negative correlation occurred at station 1, with a value of R=-0.13, while station 3 were ignored, with a correlation value of R=0.03. For the SST and SSS pair, a moderate and negative correlation was obtained at station 10 with a value of R=-0.6. Weak and negative

correlations were observed at stations 2, 5, 6, 8, and 9 with a value of -0.14≤R≤-0.38. A weak and positive correlation was discovered at station 3, with a value of R=0.2. The correlation for stations 1, 4, and 7 were ignored because the R-value is close to zero.

CONCLUSION

The seasonal model and correlation analysis in NBoB were completed in this present study. The result is based on the fact that the three parameters, namely Chl-a, SST, and SSS, follow the monsoon pattern. Therefore, this relatively regular pattern is predictable. The occasional climate changes, such as El Nino and Indian Ocean dipole (IOD) events, which tends to cause a shift in wind direction, are a limitation. These events will, of course, affect the three parameters Chl-a, SST, and SSS. The correlation analysis also has certain limitations because it involves time series data. The CMEMS data used has a high resolution and reliability, as stated in the introduction. The Chl-a graph is relatively flat from January to May at the beginning of the year, then develops a peak in the subsequent months annually and at various stations. The Min values of Chl-a occurred in February, March, and April, while that of the Max was relatively 2 mg/m^3 at stations 1, 2, 3, 4, 5, and 7, but at stations 9 and 10, although it reached 12 to 14 mg/m^3. Besides, stations 9 and 10 were only 2° 30′ E in longitude from the other 8, meaning that their positions are extremely sensitive to changes in Chl-a values. When the SW monsoon occurs, Chl-a values reaches its Max, and this occurs in July, August, and September. The Min SST values were detected in January and in the year in virtually every station. Occasionally, there was a shift in the Min SST, from January to December. The Min SST is associated with the NE monsoon, which causes winter. The SST graph shows several peaks in the form of positive local extremes every year at virtually all stations. The Max SST occurred in May, June, and July, according to the shape of the graph. The SSS graph achieved it peak in either May or April, while the valley was observed in September and October. From the seasonal model, Chl-a and SSS graphs had 1 trough and 1 peak, respectively, while the SST graph had only 1 peak. This is because the Chl-a had a Min value at the initial chart pattern, before obtaining the Max. The SST graph had a Max value in the middle of the year, while the Min was realized at the beginning or towards the end. The SSS graph reaches the Max value and then declines to the Min. The results of the seasonal model produced a periodic curve where the peaks and troughs can be identified. The Min Chl-a value occurred in February and March, while the Max was obtained in August. The Min and Max SST values were detected in January and July, respectively. For the SSS variable, the Min values vary from August to November, depending on the station, while the Max occurred from February to May. The average correlation for Chl-a and SST parameters at 10 stations was R=0.544, indicating that the relationship is moderate and positive. The Chl-a and SST values for the 10 stations studied mutually support each other or are directly proportional. For Chl-a and SSS parameters, the average correlation was R=-0.582, and this shows that the relationship is moderate and negative. The values of Chl-a and SST are inversely related, for Instance when the Chl-a value is high, SST become low, and vice versa. The average correlation for the 10 stations studied shows a weak and negative relationship of R=-0.164 for SST and SSS parameters.

AUTHOR CONTRIBUTIONS

S. Rizal performed the literature review, experimental design, analyzed and interpreted the data, prepared the manuscript text, and manuscript edition. M.N. Hidayat performed the literature review, analyzed and interpreted the data, prepared the manuscript text, and manuscript edition. R. Wafdan performed the literature review, interpreted the data, prepared the manuscript text, and manuscript edition. M. Ramli performed the literature review, analyzed and interpreted the data, prepared the manuscript text, and manuscript edition. Z.A. Muchlisin performed the literature review, prepared the manuscript text, and manuscript edition.

ACKNOWLEDGEMENT

This research was funded by the Ministry of Education, Culture, Research and Technology of the Republic of Indonesia with the scheme “Penelitian Pendidikan Magister menuju Doktor untuk Sarjana Unggul (PMDSU)” for the 2022 fiscal year with the contract number [97/UN11.2.1/PT.01.03/DPRM/2022] and the scheme of “Penelitian Profesor (PP)” for the 2022 fiscal year with the contract number [025/UN11.2.1/PT.01.03/PNBP/2022]. This research was conducted at the Ocean Modelling Laboratory,

Department of Marine Sciences, Universitas Syiah Kuala, Indonesia.

CONFLICT OF INTEREST

The author declares that there is no conflict of interest regarding the publication of this manuscript. In addition, the ethical issues, including plagiarism, informed consent, misconduct, data fabrication and/or falsification, double publication and/or submission, and redundancy have been completely observed by the authors.

OPEN ACCESS

PUBLISHER'S NOTE

GJESM Publisher remains neutral with regard to jurisdictional claims in published maps and institutional afflictions.

ABBREVIATIONS

3D	Three-dimensional
°C	Degree Celsius
°N	Degree North
°E	Degree East
a	The slope of the regression line (regression coefficient)
b	The y-intercept constant
BGC-Argo	Biogeochemical-Argo
BoB	Bay of Bengal
Chl	Chlorophyll
Chl-a	Chlorophyll-a
Chl-b	Chlorophyll-b
Chl-a/b	Chlorophyll-a per chlorophyll-b
Chl a+b	Total chlorophyll
CMEMS	Copernicus Marine Environment Monitoring Service
ENSO	El Niño-Southern Oscillation
INS TAC	In situ thematic centre
IOD	Indian ocean dipole
m	Meter
m/s	Meter per second
mg/g	Milligram per gram
mg/m³	Milligrams per cubic meter
max	Maximum
min	Minimum
MLD	Mixed layer depth
NBoB	Northern Bay of Bengal
NCAR	National center for atmospheric research reanalysis
NCEP	National centers for environmental prediction
NE	Northeast
Pa	Pascals
psu	Practical salinity unit
R	Correlation coefficient
RMS	Root mean square
RMSE	Root mean square error
SSS	Sea surface salinity
SST	Sea surface temperature
SW	Southwest
TC	Tropical cyclone

REFERENCES

Bandyopadhyay, S.; Dasgupta, S.; Khan, Z. H.; Wheeler, D., (2021). Spatiotemporal analysis of tropical cyclone landfalls in Northern Bay of Bengal, India and Bangladesh. Asia Pac. J. Atmos. Sci., 57(4): 799-815 **(17 pages).**

Belward, A.; Bourassa, M.; Dowell, M.; Briggs, S.; Dolman, H.; Holmlund, K.; Verstraete, M., (2016). The global observing system for climate: Implementation needs. World Meteorological Organization, Switzerland **(325 pages)**.

Björn, L. O.; Papageorgiou, G. C.; Blankenship, R. E., (2009). A

viewpoint: why chlorophyll a? Photosynth. Res., 99(2): 85-98 **(14 pages).**

Bosc, C.; Delcroix, T.; Maes, C., (2009). Barrier layer variability in the western Pacific warm pool from 2000 to 2007. J. Geophys. Res., Oceans, 114: C06023 **(14 pages)**.

Chaturvedi, N. (2005). Variability of chlorophyll concentration in the Arabian Sea and Bay of Bengal as observed from SeaWiFS data from 1997–2000 and its interrelationship with sea surface temperature (SST) derived from NOAA AVHRR. Int. J. Remote Sens., 26(17): 3695-3706 **(12 pages).**

Chauhan, O.S.; Rajawat, A.S.; Pradhan, Y.; Suneethi, J.; Nayak, S.R., (2005). Weekly observations on dispersal and sink pathways of the terrigenous flux of the Ganga–Brahmaputra in the Bay of Bengal during NE monsoon. Deep Sea Res. Part II, 52(14): 2018-2030 **(13 pages).**

Choudhury, A.K.; Pal, R., (2010). Phytoplankton and nutrient dynamics of shallow coastal stations at Bay of Bengal, Eastern Indian coast. Aquat. Ecol., 44(1): 55-71 **(17 pages).**

Daqamseh, S. T.; Al-Fugara, A. K.; Pradhan, B.; Al-Oraiqat, A.; Habib, M., (2019). MODIS derived sea surface salinity, temperature, and chlorophyll-a data for potential fish zone mapping: West red sea coastal areas, Saudi Arabia. Sensors., 19(9): 2069 **(25 pages).**

Dutta, S.; Paul, S., (2021). Temporal variability of economic fish assemblage of the Northern Bay of Bengal in relation to its environment. Iran. J. Ichthyol., 8(2): 104-113 **(10 pages).**

Eyring, V.; Bony, S.; Meehl, G. A.; Senior, C. A.; Stevens, B.; Stouffer, R. J.; Taylor, K. E., (2016). Overview of the coupled model intercomparison project phase 6 (CMIP6) experimental design and organization. Geosci. Model. Develop., 9(5): 1937–1958 **(22 pages)**.

Fan, K.; Wang, X.; He, Z., (2020). Control of salinity stratification on recent increase in tropical cyclone intensification rates over the postmonsoon Bay of Bengal. Environ. Res. Lett., 15(9): 094028 (**10 pages).**

Floeter, S. R.; Guimarães, R. Z.; Rocha, L. A.; Ferreira, C. E. L.; Rangel, C. A.; Gasparini, J. L., (2001). Geographic variation in reef-fish assemblages along the Brazilian coast. Global Ecol. Biogeogr., 10(4): 423-431 **(9 pages).**

Goswami, B.N.; Rao, S.; Sengupta, D.; Chowdary, S., (2016). Monsoons to mixing in the Bay of Bengal: multiscale air-sea interactions and monsoon predictability. Oceanography. 29(2): 18–27 **(10 pages).**

Haditiar, Y.; Putri, M. R.; Ismail, N.; Muchlisin, Z. A.; Rizal, S., (2019) Numerical simulation of currents and volume transport in the Malacca Strait and part of South China Sea. Eng. J., 23(6): 129–143 **(15 pages).**

Haridhi, H.A.; Nanda, M.; Wilson, C.R.; Rizal, S., (2016). Preliminary study of the sea surface temperature (SST) at fishing ground locations based on the net deployment of traditional purse-seine boats in the northern waters of Aceh: A community-based data collection approach. Reg. Stud. Mar. Sci., 8: 114–121 **(8 pages).**

Hu, S.; Sprintall, J.; Guan, C.; Hu, D.; Wang, F.; Lu, X.; Li, S., (2020). Observed triple mode of salinity variability in the thermocline of tropical Pacific Ocean. J. Geophys. Res.: Oceans. 125(9): e2020JC016210 **(12 pages).**

Ikhwan, M.; Haditiar, Y.; Wafdan, R.; Ramli, M.; Muchlisin, Z. A.; Rizal, S., (2022). Seasonal variability of mixed layer depth in the Andaman Sea. Int. J. Environ. Sci. Technol., 19: 12437–12446 **(10 pages).**

Kalnay, E.; Kanamitsu, M.; Kistler, R.; Collins, W.; Deaven, D.; Gandin, L.; Iredell, M.; Saha, S.; White, G.; Woollen, J.; Zhu, Y.; Leetmaa, A.; Reynolds, R.; Chelliah, M.; Ebisuzaki, W.; Higgins, W.; Janowiak, J.; Mo, K. C.; Ropelewski, C.; Wang, J.; Leetmaa, A.; Reynolds, R.; Jenne, R.; Joseph, D., (1996). The NCEP/NCAR 40-year reanalysis project. Bull. Am. Meteorol. Soc., 77(3): 437–471 **(34 pages).**

Lamouroux, J.; Perruche, C.; Mignot, A.; Paul, J.; Szczypta, C., (2019). Quality information document for global biogeochemical analysis and forecast product global_analysis_forecast_bio_001_028. EU Copernicus Marine Service, European Union **(44 pages).**

Latha, T.P.; Rao, K.H.; Nagamani, P.V.; Amminedu, E.; Choudhury, S.B.; Dutt, C.B.S.; Dadhwal, V.K., (2015). Impact of cyclone phailin on chlorophyll-a concentration and productivity in the Bay of Bengal. Int. J. Geosci., 6(05): 473 **(8 pages).**

Lellouche, J.M.; Legalloudec, O.; Regnier, C.; Levier, B.; Greiner, E.; Drevillon, M., (2019). Quality information document for global sea physical analysis and forecasting product, Global_Analysis_ForecaST_PHY_001_024. EU Copernicus Marine Service, European Union **(81 pages).**

Lellouche, J.M.; Greiner, E.; Galloudec, O.L.; Garric, G.; Regnier, C.; Drevillon, M.; Traon, P.Y.L., (2018). Recent updates to the Copernicus Marine Service global ocean monitoring and forecasting real-time 1/12° high-resolution system. Ocean. Sci., 14: 1093–1126 **(34 pages).**

Le Traon, P. Y.; Reppucci, A.; Alvarez Fanjul, E.; Aouf, L.; Behrens, A.; Belmonte, M.; Bentamy, A.; Bertino, L.; Brando, V. E.; Kreiner, M. B.; Benkiran, M.; Carval, T.; Ciliberti, S. A.; Claustre, H.; Clementi, E.; Coppini, G.; Cossarini, G.; Alonso-Muñoyerro, M. D. A.; Delamarche, A.; Dibarboure, G.; Dinessen, F.; Drevillon, M.; Drillet, Y.; Faugere, Y.; Fernández, V.; Fleming, A.; Garcia-Hermosa, M. I.; Sotillo, M. G.; Garric, G.; Gasparin, F.; Giordan, C.; Gehlen, M.; Gregoire, M. L.; Guinehut, S.; Hamon, M.; Harris, C.; Hernandez, F.; Hinkler, J. B.; Hoyer, J.; Karvonen, J.; Kay, S.; King, R.; Lavergne, T.; Lemieux-Dudon, B.; Lima, L; Mao, C.; Martin, M. J.; Masina, S.; Melet, A.; Nardelli, B. B.; Nolan, G.; Pascual, A.; Pistoia, J.; Palazov, A.; Piolle, J. F.; Pujol, M. I.; Pequignet, A. C.; Peneva, E.; Gómez, B. P.; de la Villeon, L. P.; Pinardi, N.; Pisano, A.; Pouliquen, S.; Reid, R.; Remy, E.; Santoleri, R.; Siddorn, J.; She, J.; Staneva, J.; Stoffelen, A.; Tonani, M.; Vandenbulcke, L.; Schuckmann, K. V.; Volpe, G.; Wettre, C.; Zacharioudaki, A., (2019). From observation to information and users: The Copernicus Marine Service perspective. Front. Mar. Sci., 6: 234 **(22 pages).**

Li, Y.; He, N.; Hou, J.; Xu, L.; Liu, C.; Zhang, J.; Wang, Q.; Zhang, X.; Wu, X., (2018). Factors influencing leaf chlorophyll content in natural forests at the biome scale. Front. Ecol. Evol., 6: 64 **(10 pages).**

Mason, E.; Ruiz, S.; Bourdalle-Badie, R.; Reffray, G.; García-Sotillo, M.; Pascual, A., (2019). New insight into 3-D mesoscale eddy properties from CMEMS operational models in the western Mediterranean. Ocean Sci., 15(4): 1111-1131 **(21 pages).**

Miranda, J.; Lotliker, A.A.; Baliarsingh, S.K.; Jena, A.K.; Samanta, A.; Sahu, K.C.; Kumar, T.S., (2021). Satellite estimates of the long-term trend in phytoplankton size classes in the coastal waters of north-western Bay of Bengal. Oceanologia. 63(1): 40-50 **(11 pages).**

Moradi, M., (2021). Evaluation of merged multi-sensor ocean-color chlorophyll products in the Northern Persian Gulf. Cont. Shelf Res., 221: 104415 **(15 pages).**

Pisano, A.; Marullo, S.; Artale, V.; Falcini, F.; Yang, C.; Leonelli, F. E.; Santoleri, R.; Buongiorno Nardelli, B., (2020). New evidence of Mediterranean climate change and variability from sea surface temperature observations. Remote Sens., 12(1): 132 **(18 pages).**

Qi, J.; Zhang, L.; Qu, T.; Yin, B.; Xu, Z.; Yang, D.; Li, D.; Qin, Y., (2019). Salinity variability in the tropical Pacific during the Central-Pacific and Eastern-Pacific El Niño events. J. Mar. Syst., 199: 103225 **(41 pages)**.

Sahoo, B.; Bhaskaran, P.K., (2016). Assessment on historical cyclone tracks in the Bay of Bengal, east coast of India. Int. J. Climatol., 36(1): 95-109 (**14 pages**).

Sarangi, R.K.; Devi, K.N., (2017). Space-based observation of chlorophyll, sea surface temperature, nitrate, and sea surface height anomaly over the Bay of Bengal and Arabian Sea. Adv. Space Res., 59(1): 33-44 **(12 pages).**

Schober, P.; Boer, C.; Schwarte, L.A., (2018). Correlation coefficients: appropriate use and interpretation. Anesth. Analg., 126(5): 1763-1768 **(6 pages).**

Torregroza-Espinosa, A.C.; Restrepo, J.C.; Escobar, J.; Pierini, J.; Newton, A., (2021). Spatial and temporal variability of temperature, salinity and chlorophyll-a in the Magdalena River mouth, Caribbean Sea. J. South Am. Earth Sci., 105: 102978 **(13 pages).**

Vecchi, G.A.; Harrison, D.E., (2002). Monsoon breaks and subseasonal sea surface temperature variability in the Bay of Bengal. J. Clim., 15(12): 1485-1493 **(9 pages).**

Vinayachandran, P.N.; McCreary, J.J.P.; Hood, R. R.; Kohler, K.E., (2005). A numerical investigation of the phytoplankton bloom in the Bay of Bengal during northeast monsoon. J. Geophys. Res.: Oceans. 110(C12) **(14 pages).**

Woolf, D.K.; Land, P.E.; Shutler, J.D.; Goddijn-Murphy, L.M.; Donlon, C.J., (2016). On the calculation of air–sea fluxes of CO2 in the presence of temperature and salinity gradients. J. Geophys. Res. Oceans. 121: 1229–1248 **(20 pages).**

Zhang, R.H.; Busalacchi, A.J., (2009). Freshwater flux (FWF)-induced oceanic feedback in a hybrid coupled model of the tropical Pacific. J. Clim., 22(4): 853-879 **(27 pages).**

AUTHOR (S) BIOSKETCHES

Hidayat, M.N., Ph.D. Candidate, Graduate School of Mathematics and Applied Sciences, Universitas Syiah Kuala, Banda Aceh 23111, Indonesia.
- Email: *muh.nurhidayat@gmail.com*
- ORCID: 0000-0001-8727-3615
- Web of Science ResearcherID: NA
- Scopus Author ID: NA
- Homepage: https://dmas.unsyiah.ac.id/, https://m-math.unsyiah.ac.id/

Wafdan, R., M.Sc., Instructor, Department of Marine Sciences, Faculty of Marine and Fisheries, Universitas Syiah Kuala, Banda Aceh, 23111, Indonesia.
- Email: *redjawavdhan11@gmail.com*
- ORCID: 0000-0001-5574-7089
- Web of Science ResearcherID: NA
- Scopus Author ID: 57191094408
- Homepage: https://fsd.unsyiah.ac.id/wafdan/

Ramli, M., Ph.D., Professor, Department of Mathematics, Universitas Syiah Kuala, Banda Aceh 23111, Indonesia.
- Email: *marwan.math@unsyiah.ac.id*
- ORCID: 0000-0003-1225-9063
- Web of Science ResearcherID: A-2686-2017
- Scopus Author ID: 57217110324
- Homepage: http://math.unsyiah.ac.id/ind/marwan/

Muchlisin, Z.A., Ph.D., Professor, Department of Aquaculture, Faculty of Marine and Fisheries, Universitas Syiah Kuala, Banda Aceh 23111, Indonesia.
- Email: *muchlisinza@unsyiah.ac.id*
- ORCID: 0000-0002-0858-1853
- Web of Science ResearcherID: E-2317-2015
- Scopus Author ID: 55937322900
- Homepage: https://fsd.unsyiah.ac.id/muchlisinza/

Rizal, S., Ph.D., Professor, Department of Marine Sciences, Faculty of Marine and Fisheries, Universitas Syiah Kuala, Banda Aceh, 23111, Indonesia.
- Email: *srizal@unsyiah.ac.id*
- ORCID: 0000-0003-3637-2351
- Web of Science ResearcherID: V-7627-2017
- Scopus Author ID: 57211267611
- Homepage: https://fsd.unsyiah.ac.id/syamsul_rizal/

HOW TO CITE THIS ARTICLE

Hidayat, M.N.; Wafdan, R.; Ramli, M.; Muchlisin, Z.A.; Rizal, S., (2023). Relationship between chlorophyll-a, sea surface temperature and sea surface salinity. Global J. Environ. Sci. Manage., 9(3): 389-402.

DOI: 10.22035/gjesm.2023.03.03

URL: https://www.gjesm.net/article_699963.html